

# A Porous Silicon Optical Biosensor: Detection of Reversible Binding of IgG to a Protein A-Modified Surface

Keiki-Pua S. Dancil, Douglas P. Greiner, and Michael J. Sailor\*

Contribution from the Department of Chemistry and Biochemistry, The University of California, San Diego, La Jolla, California 92093-0358

Received April 30, 1999

**Abstract:** The reversibility, specificity, stability, and scaling of signal response to analyte mass were quantified for a porous silicon-based optical interferometric biosensor. The sensor system studied consisted of a thin layer (5  $\mu\text{m}$ ) of porous silicon modified with Protein A. The system was probed with various fragments of an aqueous Human IgG analyte. The sensor operates by measurement of the Fabry–Perot fringes in the white light reflection spectrum from the porous silicon layer. Molecular binding is detected as a shift in wavelength of these fringes. IgG was added to and removed from the protein A-modified surface by changing solution pH in a flow cell, and the system was found to be reversible through several on–off cycles. The molecule used to link protein A to the porous Si surface incorporated bovine serum albumin (BSA). This approach was found to completely eliminate signal due to nonspecific binding, tested by exposure of the sensor to the F(ab')<sub>2</sub> fragment of IgG (which does not bind to protein A). The linker/protein A-modified surface was also found to be stable toward oxidation in the aqueous buffer solutions used. The shift in the Fabry–Perot fringes was found to scale with the mass of analyte bound in the porous Si layer.

## Introduction

Sensitive label-free biosensors are highly desired for applications in high throughput drug discovery and disease diagnostics.<sup>1,2</sup> The advantage of working with unlabeled analytes arises mainly from the ease of sample preparation. A variety of label-free optical transduction methods have been developed, which fall primarily into two categories: optical interferometric methods (such as grating couplers,<sup>3–5</sup> interferometers,<sup>6</sup> and evanescent wave devices<sup>7,8</sup>) and surface plasmon methods (involving thin metals such as gold and silver films<sup>9,10</sup> or colloids<sup>11</sup>). Recently we reported a Fabry–Perot transduction method applied to thin films of porous silicon.<sup>12,13</sup> Porous silicon is a nanocrystalline material that can be etched into single crystal silicon substrates with a resolution of 20  $\mu\text{m}$ , making it an ideal material to integrate with conventional silicon “biochip” fabrica-

tion technologies. The porous Si films have a high surface area and they are typically a few microns thick. In this material the Fabry–Perot fringes arise from reflection off the top and bottom of the film, so the measurement is made on the volume of sample contained within the porous matrix.<sup>14</sup> Unlike surface-sensitive techniques such as surface plasmon resonance, the signal response of the porous Si sensor does not fall off with increasing surface–analyte distance, providing a theoretically more sensitive approach and allowing the use of much longer linker molecules or multiple sequential binding steps.<sup>9,15</sup>

Several key biosensor limitations are addressed in this work. Nonspecific binding (NSB), or the appearance of a signal due to weak surface binding of interferents which may be present at a much higher concentration than the analyte, is a ubiquitous problem in label-free methodologies.<sup>9</sup> Because the response of the porous Si sensor is not dependent on surface–analyte distance, we were able to incorporate a large biomolecule (bovine serum albumin, BSA) into the linker used to attach protein A to the surface, eliminating spurious signal due to NSB.

A second issue that is specific to the porous Si sensors is that of signal stability. Unless they are chemically passivated, porous Si samples oxidize in an aqueous matrix. In the best case this phenomenon can be used to amplify a signal response due to binding,<sup>12,13</sup> but for practical devices such instability is unacceptable. In the worst case, a signal may be completely obscured by the drift incurred upon oxidation of the silicon. In this work we demonstrate that our earlier report of extreme sensitivity of these films toward antibody/antigen binding<sup>12,13</sup> can be entirely interpreted as signal drift due to oxidation. Proper stabilization of the porous Si sample by, for example, ozone oxidation prior to biochemical modification has been shown to

\* To whom correspondence should be addressed.

(1) Brecht, A.; Gauglitz, G. *Sens. Actuators B* 1997, 38, 1–7.

(2) Janata, J.; Josowicz, M.; DeVaney, D. M. *Anal. Chem.* 1994, 66, 207R–228R.

(3) Bernard, A.; Bosshard, H. R. *Eur. J. Biochem.* 1995, 230, 416–423.

(4) Polzius, R.; Diessel, E.; Bier, F. F.; Bilitewski, U. *Anal. Biochem.* 1997, 248, 269–276.

(5) Piehler, J.; Brandenburg, A.; Brecht, A.; Wagner, E.; Gauglitz, G. *Appl. Opt.* 1997, 36, 6554–6562.

(6) Brecht, A.; Gauglitz, G.; Nahm, W. *Analisis* 1992, 20, 135–140.

(7) Abel, A. P.; Weller, M. G.; Duveneck, G. L.; Ehrat, M.; Widmer, H. M. *Anal. Chem.* 1996, 68, 2905–2912.

(8) Hutchinson, A. M. *Mol. Biotechnol.* 1995, 3, 47–54.

(9) Homola, J.; Yee, S. S.; Gauglitz, G. *Sens. Actuators B* 1999, 54, 3–15.

(10) Nikitin, P. I.; Beloglazov, A. A.; Kochregina, V. E.; Valeiko, M. V.; Ksenevich, T. I. *Sens. Actuators B* 1999, 54, 43–50.

(11) Lyon, L. A.; Musick, M. D.; Natan, M. J. *Anal. Chem.* 1998, 70, 5177–5183.

(12) Janshoff, A.; Dancil, K.-P. S.; Steinem, C.; Greiner, D. P.; Lin, V. S.-Y.; Gurtner, C.; Motesharei, K.; Sailor, M. J.; Ghadiri, M. R. *J. Am. Chem. Soc.* 1998, 120, 12108–12116.

(13) Lin, V. S.; Motesharei, K.; Dancil, K. S.; Sailor, M. J.; Ghadiri, M. R. *Science* 1997, 278, 840–843.

(14) Curtis, C. L.; Doan, V. V.; Credo, G. M.; Sailor, M. J. *J. Electrochem. Soc.* 1993, 140, 3492–3494.

(15) Gauglitz, G.; Brecht, A.; Kraus, G.; Nahm, W. *Sens. Actuators B* 1993, 11, 21–27.

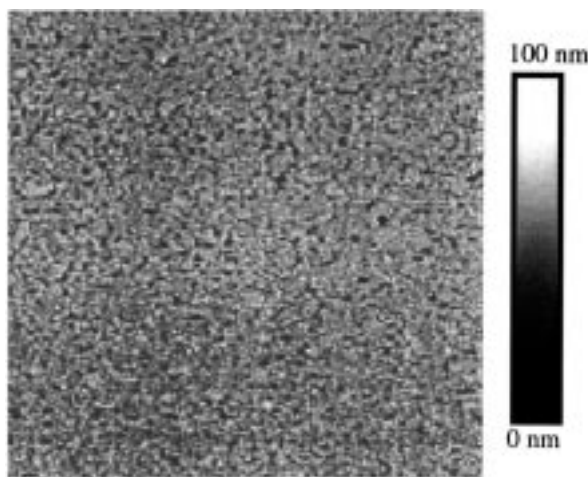


**Figure 1.** TappingMode atomic force microscope image ( $5 \times 5 \mu\text{m}$ ) of a freshly etched porous Si sample of the type used in this study. The current density used in the etch is  $500 \text{ mA/cm}^2$ . Pores are 100–300 nm in diameter. The vertical bar shows the mapping of the sample height (in nm) onto the gray scale used to display the image, to aid in visualizing depth of the features.

reduce signal drift to acceptable levels.<sup>12</sup> It is found in this work that incorporation of BSA in the linker further stabilizes the porous Si layer by at least a factor of 50.

Finally, scaling of the signal response with analyte mass is addressed in this work. Although the theory of operation of the porous Si Fabry–Perot sensors has been developed in some detail<sup>12</sup> the expected relationship between signal change and analyte mass has not previously been experimentally verified. In this work we have quantified the shift in effective optical thickness (EOT) derived from analysis of the reflectivity spectra for bound streptavidin (MW 67 kDa), biotinylated protein A (MW 42 kDa), IgG (MW 150 kDa), and the  $F_c$  fragment of IgG (MW 50 kDa).

## Results and Discussion

**Pore Characterization.** The dimensions of the pores generated in the electrochemical etch used to make porous silicon have been shown to display a complex relationship between current density, electrolyte composition, and wafer dopant type and resistivity.<sup>16</sup> It has been found that etching  $p^+$  wafers generally produces pores on the order of 5 nm in diameter. These are too small to allow access of large molecules such as antibodies. For example, the spheroid dimensions of human IgG are 3 nm by 15 nm.<sup>17</sup> The preparation used in our earlier work generates pores of  $<5$  nm diameter (by atomic force microscopic analysis), and test experiments with concentrated BSA solutions (MW of BSA is 67 kDa) confirm that the pores are too small to allow entry of the molecules of interest.<sup>13</sup> In a subsequent work a method was developed to generate pores with acceptable dimensions (tunable between 5 and 1200 nm) using highly degenerate  $p^{++}$  wafers, and this method was used to produce the samples in the present study. Figure 1 shows a plan-view TappingMode atomic force microscope (AFM) image representative of the porous Si samples used. Pores ranging from 100 to 300 nm in diameter are evident. The thickness of the porous matrix was determined by profilometry to be  $5 \mu\text{m}$ .

**Surface Modification.** Several issues were addressed in designing the linker for sensing biochemical interactions within

the porous layer: (1) stability in aqueous environments, (2) accessibility of the recognition elements to the incoming analytes, and (3) hydrophilicity (minimization of nonspecific binding). The chemistry used is outlined in Scheme 1. The first step involves oxidation/hydroxylation of the hydride-terminated porous Si surface. The reaction is performed by exposing the freshly etched porous Si sample (1) to a flowing stream of ozone for 70 s. Infrared spectra of the porous Si sample indicate that the reaction produces a hydroxylated silicon oxide layer (2) on top of the porous Si matrix. Trace A in Figure 2 shows the diffuse reflectance FT-IR spectrum of the ozone-oxidized porous Si sample. A large Si–O–Si vibrational band at  $1100 \text{ cm}^{-1}$  is apparent. A band assigned to a  $\delta_{\text{Si-OH}}$  vibrational mode is observed at  $880 \text{ cm}^{-1}$ .

Condensation of the Si–OH surface species (2) with 2-pyridyldithio(propionamido)dimethylmonomethoxysilane generates a surface-bound pyridyldithio group (3). The infrared spectrum of this modified material (Figure 2, trace B) displays the characteristic amide I  $\nu_{\text{C=O}}$  ( $1647 \text{ cm}^{-1}$ ), amide II  $\delta_{\text{N-H}}$ ,  $\nu_{\text{N-C=O}}$  ( $1550 \text{ cm}^{-1}$ ), broad amide A  $\nu_{\text{N-H}}$  ( $3290 \text{ cm}^{-1}$ ), aliphatic  $\nu_{\text{C-H}}$  ( $2959$ ,  $2930$ , and  $2860 \text{ cm}^{-1}$ ), and aromatic  $\nu_{\text{C-H}}$  ( $3067 \text{ cm}^{-1}$ ) vibrational bands indicative of the surface-attached pyridyldithio(propionamido) species.<sup>18</sup>

Reaction of the pyridyldithio-modified surface (3) with dithiothreitol (DTT) results in reduction of the disulfide bond, releasing 2-thiopyridone and generating an attached S–H species (4). The amount of 2-thiopyridone released was quantified by UV–visible absorption spectroscopy ( $\lambda_{\text{max}} = 343 \text{ nm}$ ,  $\epsilon = 8.03 \times 10^3 \text{ M}^{-1} \text{ cm}^{-1}$ ).<sup>19</sup> The amount of 2-thiopyridone detected provides a measurement of the number of sulfhydryls available for receptor molecule attachment. From the measured concentration of 2-thiopyridone released it was calculated that the porous material under a  $1 \text{ mm}^2$  sensing area contains approximately  $3.4 \times 10^{-10} \text{ mol}$  of receptor molecules.

The sulfhydryl-terminated material (4) was then quickly mounted in the Plexiglas flow cell used in the optical reflectivity measurements. The cell was filled with the *N*- $\gamma$ -maleimidobutyryloxysuccinimide ester (GMBS) solution to allow coupling of the sulfhydryl group with the maleimide group rendering a NHS-modified surface (5). The cell was then flushed with PBS solution containing 10% ethanol to remove the reaction byproducts and the unreacted GMBS reagent. After 30 min of rinsing with alcoholic PBS, the solution in the flow cell was replaced with a completely aqueous PBS buffer solution and an initial measurement of the Fabry–Perot fringes was performed.

The cell was then flushed with a solution containing biotinylated bovine-serum albumin, which couples to the NHS-modified porous Si surface (5). A BSA incorporated linker surface (6) was established. An increase in the effective optical thickness (EOT) of the Fabry–Perot layer was observed, indicative of a change in refractive index induced by binding of the biotinylated BSA into the composite film. Addition of biotinylated BSA results in a change in EOT of 100 nm (from 8390 to 8490 nm). This large increase is attributed to two factors. First, replacement of some of the aqueous phase (approximate refractive index 1.33) with protein (approximate refractive index 1.42)<sup>20</sup> will change the mean refractive index of the film and be observed as an increase in EOT. The second factor that

(18) Pretsch, E.; Simon, W.; Seibl, J.; Clerc, T. *Tables of Spectral Data for Structural Determination of Organic Compounds*, 2nd ed.; Springer-Verlag: Berlin, 1989.

(19) Hermanson, G. T. *Bioconjugate Techniques*; Academic Press: San Diego, 1996; p 785.

(20) Spaeth, K.; Brecht, A.; Gauglitz, G. *J. Colloid Interface Sci.* **1997**, *196*, 128–135.

(16) Herino, R. Pore Size Distribution in Porous Silicon. In *Properties of Porous Silicon*; Canham, L., Ed.; Short Run Press Ltd.: London, 1997; Vol. 18, pp 89–96.

(17) Valentine, R. C.; Green, N. M. *J. Mol. Biol.* **1967**, *27*, 615–617.

Scheme 1

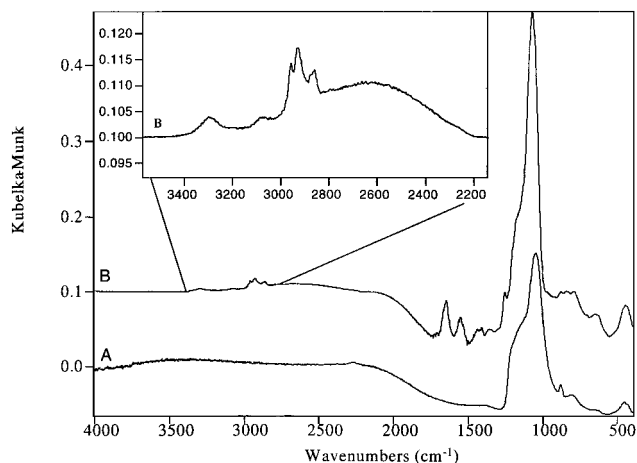
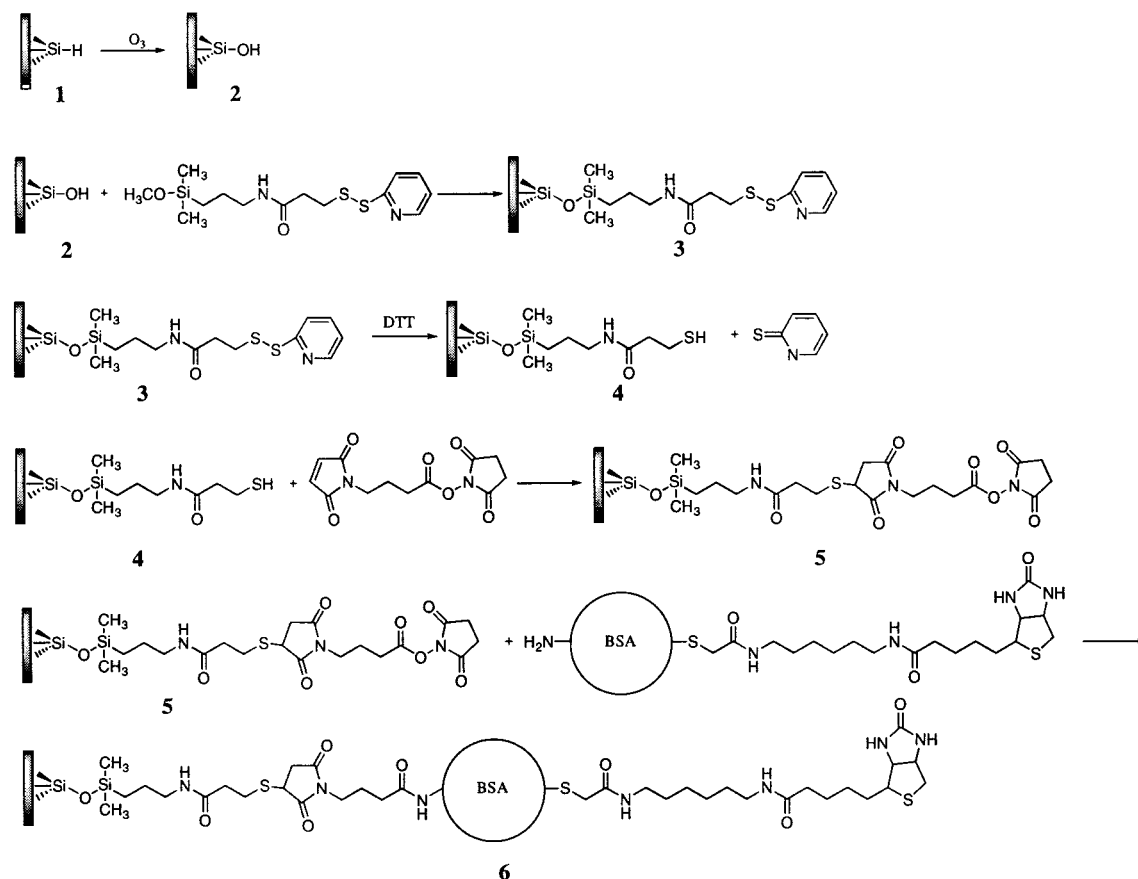


**Figure 2.** FT-IR diffuse reflectance spectra of an ozone oxidized porous Si sample (trace A) and after derivatization with (2-pyridyldithiopropanamido)dithiopyridinemonomethoxysilane (trace B). The inset shows an expansion of trace B in the N-H and C-H stretching region, showing the amide A (N-H), aromatic (C-H), and aliphatic (C-H) bands.

contributes to the increase is ascribed to wetting of the porous Si layer, presumably replacing trapped air bubbles in the film with the aqueous phase. Once the hydrophilic BSA linker is attached (6), wetting is complete and any additional changes in EOT arise from only the first factor. Consequently, binding of any additional biomolecules will lead to a change in EOT that directly scales with analyte mass (see below). At this stage the surface was rinsed thoroughly with PBS buffer to ensure covalent attachment to the surface and to check stability of the EOT measurement.

**Stability in Aqueous Buffer Solution.** Biological interactions take place in aqueous environments usually at physiological pH. Therefore, the porous Si chips must be stable under these conditions to serve an analytically useful function. As previously reported, porous Si displays various degrees of stability in aqueous media depending on the surface preparation.<sup>12</sup> Oxidation of an unprotected porous Si layer will generally lead to a blue shift of the Fabry-Perot fringes as the Si in the film is converted to  $SiO_2$ . A blue shift observed upon bioanalyte binding to porous Si films was originally interpreted as a modification of carrier density in the nanocrystalline Si material, similar to the Franz-Keldysh effect.<sup>13</sup> It is now apparent that the original interpretation was in error, and the results can be attributed to oxidation or dissolution of the porous Si surface.

The extent of oxidation of various surface preparations was quantified in the present study, and is summarized in Figure 3. If a sample with the surface preparation used in our earlier work<sup>13</sup> (bromine oxidation and a trimethoxy silane linker) is placed in aqueous PBS containing 10% ethanol (v/v), the rate of change in EOT is 2.4 nm/min (Figure 3, trace A). In an aqueous 0.5 M NaCl medium (the solution used in the prior antibody biosensor study),<sup>13</sup> the rate of change in EOT is quite variable but averages 3.2 nm/min (Figure 3, trace B). The measured background drift rate of these samples is comparable to the change in signal with time that was reported in the antibody/antigen sensing study.<sup>13</sup> Thus the present results suggest that the signal change ascribed to antigen binding in the previous work can be completely attributed to drift due to sample oxidation by the aqueous media. The main conclusion that can be drawn from these data is that oxidation can overwhelm any useful signal that might be obtained on nonstabilized samples. Under the appropriate conditions, oxidation that is

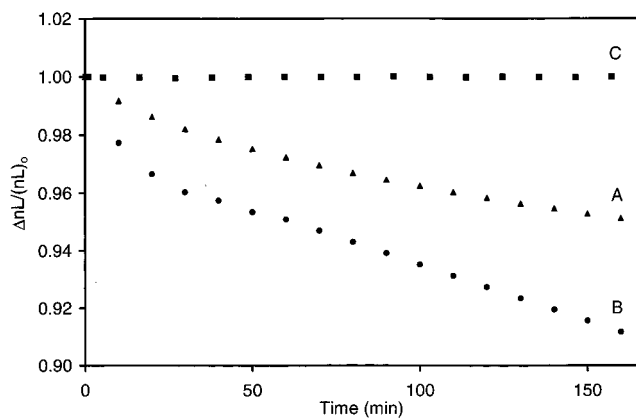


**Figure 3.** Relative change in effective optical thickness of porous Si films as a function of time in aqueous solutions, demonstrating the relative stability of various preparations (slope of EOT vs time curve is given in brackets). Porous Si prepared as in ref 13 containing a trimethoxysilane linker in 10% (v/v) EtOH in PBS at pH 7.4 ( $\blacktriangle$ , A) {2.4 nm/min}. Porous Si prepared as in ref 13 containing a trimethoxysilane linker in 0.5 M NaCl ( $\bullet$ , B) {3.2 nm/min}. Porous Si of the type and preparation used in the present work containing the BSA protein-incorporated linker used in the present study in PBS at pH 7.4 ( $\blacksquare$ , C) {<0.001 nm/min}. The curve designated as B corresponds to the preparation and sample matrix conditions used in ref 13 but without attached antibody. The data show the significant background drift that can be observed without the proper passivating surface chemistry.

triggered by or enhanced by analyte binding can in principle be used to amplify a recognition event,<sup>12</sup> although care must be taken to exclude any interferents (such as peroxides or biological oxidants) that can lead to false positives.

A convenient method for stabilizing porous Si toward oxidation in aqueous environments has been reported previously.<sup>12</sup> The method involves an initial oxidation with ozone followed by modification with the biochemical linker. The preparation was found to give a background oxidation (drift) rate of only 0.05 nm/min, which is acceptable for analyses involving changes in EOT of 1 nm or more. In the present work we attempted to improve the background drift rate by incorporating a large protective protein (BSA) into the linker. The protein-incorporated linker provided the most stable surface measured, exhibiting a background drift rate of less than 0.001 nm/min in PBS buffer, Figure 3, trace C. A comparable drift rate (not shown) was obtained for PBS buffer containing 10% ethanol (v/v). This new preparation proved to be adequately stable for the present experiments, which included runs involving the sequential addition of multiple analytes and large changes in solution pH or alcohol concentration.

**Binding and Release of IgG to the Protein A-Modified Material.** Exposure of the functionalized porous Si films to various analytes results in a predictable increase in EOT, Figure 4. Because most proteins possess a relatively constant refractive index of 1.42, the change in EOT is a direct measure of the molecular weight of bound protein. The protein displaces the aqueous phase in the pores of the material upon binding, and since the refractive index of water is 1.33, protein binding results in a net increase in EOT, or a red shift in the Fabry-Perot fringes. The biotinylated surface, as prepared in Scheme 1, was exposed to flowing PBS buffer solution to establish a baseline (Figure 4, point A). Upon introduction of a solution containing 1 mg/mL of streptavidin an increase in EOT of 17 nm was observed (Figure 4, point B). Rinsing with PBS buffer at this point (Figure 4, point C) showed no change in EOT. Subsequent introduction of a solution containing 2.5 mg/mL of biotinylated Protein A (b-Prot A) resulted in an increase in EOT of 14 nm

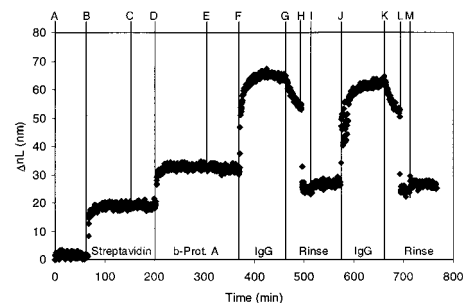


**Figure 4.** Binding curve demonstrating reversibility as well as the mass correlation of the porous Si sensor functionalized as described in Scheme 1 {change in EOT ( $\Delta nL$ ) relative to the baseline immediately before each protein addition given in brackets}: A, PBS buffer at pH 7.4; B, 1 mg/mL of streptavidin {17 nm}; C, PBS rinse; D, 2.5 mg/mL of biotinylated Protein A {14 nm}; E, PBS rinse; F and J, 2.5 mg/mL of Human IgG {34 nm}; G and K, PBS rinse; H and L, 0.1 M acetic acid; and I and M, PBS rinse. All data were acquired under a constant peristaltic flow of 0.5 mL/min in a flowcell.

(Figure 4, point D). Protein A specifically binds to the  $F_c$  region of IgG with a binding constant of  $10^8 \text{ mol}^{-1}$ .<sup>21</sup> After a PBS rinse (Figure 4, point E) introduction of a solution containing 2.5 mg/mL of Human IgG results in a further increase in EOT of 34 nm (Figure 4, point F). The observed change in EOT for binding of IgG required several minutes to reach a steady state value, presumably due to slow diffusion of this large molecule into the pores of the porous Si film. This is evident in the binding curve of Figure 4 at point F and also at point J (the replicate run with IgG, see below). At the time indicated by point G in Figure 4 the cell was flushed with PBS buffer. A slow decrease in EOT with time was observed, interpreted as dissociation of the Protein A/IgG complex. Protonation of the binding sites on protein A by decreasing the pH of the solution releases IgG from protein A.<sup>19</sup> Thus switching the solution in the flow cell to a solution containing 0.1 M acetic acid (pH 2.78) resulted in an almost instantaneous decrease of EOT close to a level corresponding to uncomplexed protein A (Figure 4, point H). A subsequent rinse with PBS returned the value of EOT to the value measured before introduction of IgG (Figure 4, point I). A slight increase in EOT is observed upon replacing the acetic acid solution with PBS buffer solution because the refractive index of the acetic acid solution is less than the index of the PBS buffer solution. A replicate IgG binding/release run was then performed to measure reproducibility of the method (Figure 4, points J–M), which gave good agreement with the original.

**Tests for Nonspecific Interactions.** Previous Biotin/Streptavidin experiments were conducted in PBS buffer (pH 7.4) containing 0.1% of the detergent Triton X-100.<sup>12</sup> The detergent was used to reduce false signals caused by nonspecific binding at the porous Si surface. To eliminate the necessity for detergent in the analyte solution, bovine serum albumin (BSA) was incorporated into the linker (Scheme 1). It was hoped that by incorporating BSA the hydrophilicity of the porous material would be increased to the point that a carrier protein or detergent would no longer be necessary. A second reason for incorporating BSA into the linker was to separate binding sites in the porous Si films. In earlier work we found that the response of the porous Si sensors did not scale with mass of analyte as expected, consistently underestimating the mass of larger analytes.<sup>22</sup> The

(21) Lindmark, R.; Thoren-Tolling, K.; Sjoquist, J. *J. Immunol. Methods* **1983**, *62*, 1–13.

(22) Dancil, K.-P. S.; Greiner, D. P.; Sailor, M. J. In *Materials Research Society Symposium Proceedings*; Canham, L. T., Sailor, M. J., Tanaka, K., and Tsai, C.-C., Eds.; Boston, MA, 1999; Vol. 536, pp 557–562.

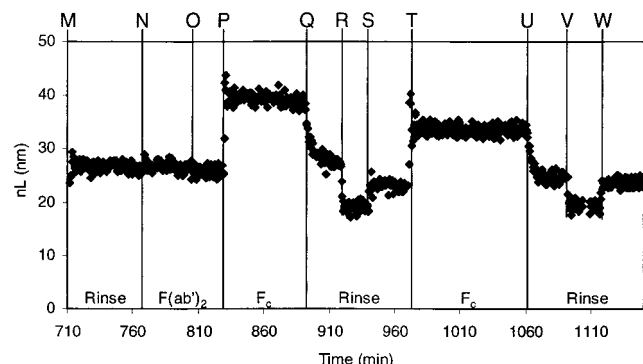


**Figure 5.** Binding curve continuing from Figure 4 showing the insensitivity of the system to nonspecific interactions at the third protein layer on the sensor surface {change in EOT ( $\Delta nL$ ) relative to the baseline immediately before each protein addition given in brackets}: M, PBS rinse; N, 2.5 mg/mL of Human IgG,  $F(ab')_2$  fragment {0 nm}; O, PBS rinse; P and T, 2.5 mg/mL of Human IgG  $F_c$  fragment {13 nm}; Q and U, PBS rinse; R and V, 0.1 M acetic acid; and S and W, PBS rinse.

results were interpreted as a crowding of binding sites at the surface. For the present work, it was thought that incorporation of BSA (15 nm diameter) into the linker would serve to space the protein binding sites further apart, minimizing the possibility that IgG bound to one site would block neighboring binding sites.

IgG is susceptible to proteolytic attack by enzymes such as pepsin and papain.<sup>23</sup> Cleavage at the hinge region of IgG produces fragments known as  $F_c$  and either  $F(ab')_2$  or  $F(ab)$  depending upon the enzyme used. The  $F_c$  fragment contains the binding domain recognized by protein A. The  $F(ab')_2$  or  $F(ab)$  fragments contain the antigen binding regions and do not bind specifically to protein A. The response of the protein A-modified sensor was tested with both the  $F(ab')_2$  and  $F_c$  fragments of IgG. Figure 5 shows the data from a continuation of the binding run of Figure 4. The PBS buffer baseline at point M in Figure 5 is identical to point M in Figure 4. Upon introduction of a solution of 2.5 mg/mL of the  $F(ab')_2$  fragment of Human IgG no change in EOT was observed (Figure 5, point N). A buffer rinse following introduction of the nonspecific  $F(ab')_2$  fragment also resulted in no change in EOT (Figure 5, point O). Addition of 2.5 mg/mL of the  $F_c$  fragment of Human IgG resulted in an increase in EOT of 13 nm (Figure 5, point P). Reversibility was also investigated by cycling the  $F_c$  fragment on (Figure 5, points P and T) and off (Figure 5, points Q–S and U–W) the surface in a fashion similar to the IgG binding runs of Figure 4. Similar results were observed. Although a slight drift in EOT (blue shift of 0.01 nm/min) due to background oxidation was observed in the experiments, the changes in EOT measured immediately before reagent introduction and after achievement of the steady-state responses were consistent throughout the runs.

The changes in EOT upon binding and release of the  $F_c$  fragment typically required less time to reach their steady-state values than was observed for binding and release of the intact IgG molecule, as can be seen in the traces of Figures 4 and 5. The time response of the data is thought to arise from a combination of the protein association (or dissociation) rate constants and the diffusional characteristics of the molecules in the pores of the sensing matrix. The rate constants for the  $F_c$  fragment and intact IgG should be approximately the same, so the decreased response time for the  $F_c$  fragment relative to IgG

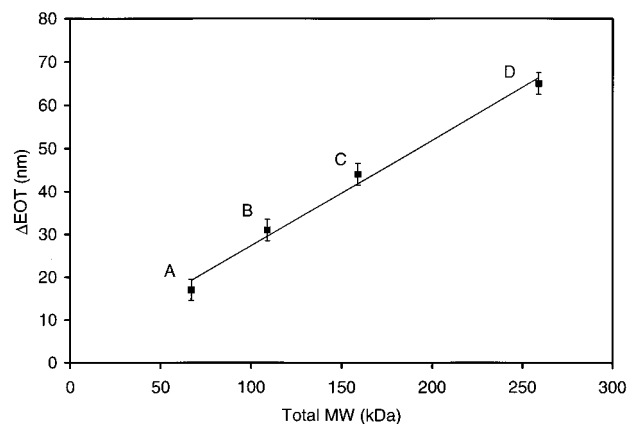


**Figure 6.** Overall change in EOT of the porous Si sensor as a function of total MW of protein complex bound to the inner pore walls: A, streptavidin (67 kDa); B, streptavidin/b-Prot A (109 kDa); C, streptavidin/b-Prot A/ $F_c$  fragment (159 kDa); and D, streptavidin/b-Prot A/Human IgG (259 kDa). The points are not listed in order of introduction to the sensor.

presumably arises from the smaller size of the  $F_c$  fragment. The  $F_c$  fragment is expected to have a correspondingly larger diffusion coefficient in the confines of the porous Si matrix. It is not clear at this time if reliable kinetic constants can be extracted from such data.

**Correlation of Effective Optical Thickness (EOT) with Analyte Mass.** The total molecular weight (MW) of bound protein (analyte) displays a linear correlation with the change in EOT observed, Figure 6. Binding of streptavidin, with a MW of 67 kDa, increases the total EOT by 17 nm (Figure 6, point A). Addition of biotinylated protein A increases EOT by 14 nm, corresponding to a net change in EOT of 31 nm for the streptavidin/b-Prot A complex (total MW of 109 kDa, Figure 6, point B). Binding of the  $F_c$  fragment to the streptavidin/b-Prot A complex (Figure 6, point C) increases the total bound MW to 159 kDa, corresponding to a 13 nm increase in EOT (net 44 nm). The total MW for the streptavidin/b-Prot A complex with human IgG is 259 kDa, and the net change in EOT is 65 nm (Figure 6, point D). The correlation of molecular weight to EOT follows a line with a slope of 0.25 nm/kDa. These data demonstrate that the sensor response scales with the mass of the analyte. With the experimental configuration, spectrometer, and data analysis used in these experiments, reliable data can be obtained for analyte masses above ca. 20 kDa.

## Conclusions

We have investigated the use of porous Si as an immobilization and transducing matrix for monitoring protein–protein binding, specifically protein A with IgG. Transduction was achieved by monitoring the change in effective optical thickness (EOT) of a functionalized porous Si Fabry–Perot film upon analyte binding. Sensor stability, reversibility, insensitivity to nonspecific interactions, and the correlation of signal response with analyte mass were demonstrated in this study.

Stability of the silicon substrate material toward oxidation was improved significantly. Control experiments on the type of nonstabilized porous Si films used in our earlier antibody/antigen binding study<sup>13</sup> were performed. The data indicate that drift due to background oxidation by the aqueous matrix can account for all of the signal change that was originally attributed to analyte binding.<sup>13</sup> A combination of ozone oxidation of the porous Si substrate material and the incorporation of a hydro-

philic protein into the linker improved stability in aqueous environments sufficiently to allow detection of molecular interactions without introducing any significant signal drift.

Detection of binding events occurring far from the silicon surface was achieved (several protein layers). The system was easily able to detect binding of IgG and the Fc fragment of IgG to protein A tethered to the porous Si surface through a modified BSA–biotin–streptavidin linker. Reversibility of the system was demonstrated by sequential addition and removal of IgG. IgG was removed by protonation of the protein A binding site with acetic acid. Elimination of spurious signals from nonspecific interactions was achieved by incorporating bovine serum albumin into the linker used to immobilize the protein to the porous Si surface. The effect of nonspecific binding was tested with the F(ab')<sub>2</sub> and Fc fragments of IgG. A change in effective optical thickness only occurred upon introduction of the Fc fragment (or the intact IgG protein). This interaction was also reversible. A linear correlation between change in EOT and mass of introduced analyte was demonstrated.

## Experimental Section

**Etching Procedure.** Porous Si samples were prepared by anodically etching p<sup>++</sup>-type silicon (0.6–1.0 mΩ·cm resistivity, (100) orientation, B-doped, International Wafer Service) in an ethanolic HF solution (HF–ethanol 3:1, v/v) at 500 mA/cm<sup>2</sup> for 10 s in the dark. A Pt mesh counter electrode was used to ensure a homogeneous electric field. Each sample was rinsed thoroughly with ethanol and methylene chloride and then dried under a stream of nitrogen.

**Characterization of Porous Si Morphology.** Atomic force microscopy (AFM) images were obtained under ambient conditions using a Nanoscope IIIa Multimode scanning probe microscope (Digital Instruments, Santa Barbara, CA) operating in TappingMode to investigate pore size. The porous Si layers were dissolved in 1 M aqueous NaOH and profiles were obtained with a Dektak II Profilometer (Veeco/Sloan Technology, Santa Barbara, CA) to determine the thickness of the films.

**Fourier Transform Infrared (FT-IR) Spectroscopy.** FT-IR spectra were acquired with a Nicolet Model 550 Magna Series II FT-IR spectrometer operating in diffuse reflectance mode. The FT-IR sample compartment was purged with nitrogen before each acquisition.

**Interferometric Reflectance Spectra.** Interferometric reflectance spectra of porous Si were obtained using an Ocean Optics fiber optic spectrometer S 2000 (Ocean Optics, FL). A tungsten light source was focused to a spot size of approximately 1 mm<sup>2</sup> on the porous Si surface.

A CCD detector operating in the range of 400–1000 nm acquired spectra every 30 s. The illumination and detection of the reflected light was performed using an incident angle of 0° to the surface normal. Values of EOT were obtained directly from a fast Fourier transform of the Hanning-modified reflectance spectra.

**Derivatization of the Porous Si Layer.** Freshly etched samples were exposed to ozone for 70 s using an ozone generator (Ozomax, Quebec, Canada) with a flow rate of 8 g/h of O<sub>3</sub> to provide an oxidized, silanol-terminated surface for further functionalization. SPDP, *N*-succinimidyl 3-(2-pyridyldithio)propionate (Pierce Chemical) (1.6 × 10<sup>-4</sup> mol) was dissolved in 20 mL of methylene chloride and 4-aminobutyldimethylmethoxysilane (Fluka Chemical) (1.6 × 10<sup>-4</sup> mol) was added slowly with stirring. The reaction was allowed to proceed overnight at room temperature. The product was purified via silica gel column using ethyl acetate as the eluent. The purified bifunctional linker was dissolved in 20 mL of toluene and was covalently attached to the oxidized porous Si surface by overnight reflux. The functionalized porous Si samples were characterized by FT-IR. The surface was then treated with 10 mM dithiothreitol, DTT (Aldrich Chemical), containing 10% ethanol for 30 min rendering a free sulfhydryl surface. *N*-γ-Maleimidobutyryloxysuccinimide ester (10 mM), GMBS (Calbiochem), was then introduced to the surface via a flowcell. The samples were rinsed with phosphate buffered saline (PBS) at pH 7.4 containing 10% ethanol initially to ensure wetting of the hydrophobic surface and to establish a baseline for the EOT measurements, then rinsed with completely aqueous PBS. Aqueous biotinylated bovine serum albumin (b-BSA) was prepared by procedures previously published.<sup>19</sup> After a baseline was established in the reflectivity spectrum, 4 mg/mL of b-BSA was introduced at a flow rate of 0.5 mL/min. An increase in EOT was observed characteristic of binding.

**Proteins.** Streptavidin and biotinylated protein A (b-Prot A) were purchased from Pierce Chemical. Human IgG, Human IgG, F(ab')<sub>2</sub> fragment, and Human IgG, Fc fragment, were purchased from Calbiochem. Each protein was diluted to the desired concentration in PBS buffer at pH 7.4. Protein was introduced into the flowcell at a flow rate of 0.5 mL/min. After each addition of protein a PBS rinse cycle was performed.

**Acknowledgment.** K.-P.S.D. would like to thank MBRS and NIH for a predoctoral fellowship (2S06GM47165-06). This work was funded by the Office of Naval Research (N0001495-11293) and the Defense Advanced Research Projects Agency (N66001-98-C-8514).

JA991421N